Journal of Solid State Chemistry 187 (2012) 264–268

Contents lists available at SciVerse ScienceDirect

Journal of Solid State Chemistry

journal homepage: www.elsevier.com/locate/jssc

Two new ternary lanthanide antimony chalcogenides: $Yb_4Sb_2S_{11.25}$ and $Tm_4Sb_2Se_{11.68}$ containing chalcogenide Q^{2-} and dichalcogenide $(Q_2)^{2-}$ anions

Jean-Marie Babo, Thomas E. Albrecht-Schmitt*

Department of Civil Engineering and Geological Sciences and Department of Chemistry and Biochemistry, University of Notre Dame, Notre Dame, IN 46556, USA

ARTICLE INFO

Article history:
Received 20 September 2011
Received in revised form
5 January 2012
Accepted 9 January 2012
Available online 20 January 2012

Keywords:
Lanthanide chalcogenides
Lanthanide antimony chalcogenides
Flux synthesis
Tunnel structure
Lone-pair effects

ABSTRACT

Dark red and dark brown crystals of $Yb_4Sb_2S_{11.25}$ and $Tm_8Sb_4Se_{11.68}$, respectively, were obtained from the reaction of the elements in Sb_2Q_3 (Q=S, Se) fluxes. Both *non*-stoichiometric compounds are orthorhombic and crystallize in the same space group *Pnnm*, with two formula units per unit cell (a=12.446(2), b=5.341(1), c=12.058(2) for sulfide and a=13.126(2), b=5.623(1), c=12.499(2) for the selenide). Their crystal structures are dominated by lanthanide-chalcogenide polyhedra (CN=7 and 8), which share corners, edges, triangular- and square-faces to form a three-dimensional framework embedding antinomy cations. The latter are coordinated by three sulfide anions with 5(1+2+2) secondary contacts forming basically infinite chains running along [0 1 0]. The chalcogens in both compounds form chalcogenide Q^{2-} and dichalcogenide $(Q_2)^{2-}$ anionic units. The optical analysis made on those compounds shows that both are semiconductors with band gap of 1.71 and 1.22 eV for $Yb_4Sb_2S_{11.25}$ and $Tm_4Sb_2Se_{11.75,}$ respectively.

1. Introduction

Compounds containing antimony and chalcogens have been intensely studied since the thermoelectric properties of Bi_2Te_3/Sb_2Te_3 were first highlighted [1]. Except some oxide and fluoro-chalcogeno–antimonates, common multinary antimony–chalcogenides exhibit the +3 oxidation state [2–8], contrary to arsenic showing regularly both +3 and +5 [9–14], while bismuth is nearly exclusively +3 in chalcogenides [15–18]. In their +3 oxidation state, the activity of stereochemical s^2 lone pair of electrons decreases as one goes from arsenic to bismuth generating structures diversity of the resulting compounds. Trivalent arsenic is between three and five coordinate, while the equivalent antimony compounds vary up to six coordinate. Many quaternary main group chalcogeno–arsenates(V) and chalcogeno –antimonates(V) have been reported while, the ternary counterpart containing lanthanides are more prevalent with divalent cations [19–20]. As chalcogeno–arsenate(III) and chalcogeno–antimonite(III) representatives containing trivalent lanthanide, few ($Pr_4S_3[AsS_3]_2$ [21], $Pr_8Sb_2S_{15}$ [22], Nd_3SbS_6 [23], $Ce_3Sb_3S_{10}$ [23] and $La_7Sb_9S_{24}$ [24] for ternary, and $Ln_2Mn_3Sb_4S_{12}$ (Ln=Pr, Nd, Sm, Gd) [25], $La_4FeSb_2S_{10}$ [26], the disordered $K_2Ln_{2-x}Sb_{4+x}Se_{12}$ (Ln=La–Pr, Gd) [27] and $K_2Gd_2Sb_2Se_9$ (Ln=La, Gd) [28] for quaternary) have been reported in literature. Many of the divalent as well as trivalent lanthanide–antimony chalcogenides likely contain polychalcogenides, which may be a factor in their stability. Additionally, all the reported trivalent (Ln^{3+}) ones are for the light lanthanides. The disordering of antimony cations in the compounds $K_2Gd_2Sb_2Se_9$ and $K_2La_2Sb_2S_9$ [28] were reported, with a structural consequence of sub- and super-structures found for both compounds.

Molten polychalcogeno–antimonate salts as flux have been used as the most successful synthetic route for the chalcogeno–antimonates(V and III) syntheses [29,30]. Here we report the synthesis, crystal structure and optical properties of the first two ternary antimony–chalcogenides of heavy trivalent lanthanides, containing chalcogenide Q^{2-} and dichalcogenide $(Q_2)^{2-}$, with two different behavior for the antimony cations.

2. Experimental

2.1. Synthesis

The following reagents were used as obtained and were stored under argon-atmosphere: Ytterbium (99.9%, Alfa-Aesar), thulium (99.9%, Alfa-Aesar), antimony (99.5%, Alfa-Aesar), sulfur (99.5%, Alfa-Aesar), selenium (99.5%, Alfa-Aesar), NaBr (99.9%, Alfa-Aesar). The Sb_2Q_3 (Q=S, Se) were prepared by heating stoichiometric mixture of antimony and chalcogen at 800 °C for three days.

The ytterbium compound was isolated during an attempt to prepare Ce_2CuYbS_5 where we have mixed the elements

* Corresponding author.
E-mail address: talbrec1@nd.edu (T.E. Albrecht-Schmitt).

0022-4596/$ - see front matter © 2012 Elsevier Inc. All rights reserved.
doi:10.1016/j.jssc.2012.01.020

stoichiometrically, with excess of Sb, S and NaBr expecting to form mixed NaBr/Sb_2S_3(with the latter produced in-situ) flux. The chemicals were loaded in a silica-glass ampoule, which was evacuated, sealed, and then was heated at 900 °C in a furnace followed by cooling at the rate of 10 °C/h to the room temperature. The $Yb_4Sb_2S_{11.25}$ compound was a by-product with an estimated yield of 8%. We have tried to synthesize this compound by mixing the stoichiometric amount of elements with NaBr as flux unsuccessfully, but instead isolated the two binary products: Yb_2S_3 and Sb_2S_3. Another possibility was to mix the elements Yb and S together with Sb_2S_3 or Yb_2S_3 and elements Sb and S, but it as well was unsuccessful. By repeating the first synthetic route using Sb_2S_3 instead of elements, but in stoichiometric amount with an excess of NaBr as flux, we were able to increase the yield to 25%. While this product together with Sb_2S_3 [31], $Ce_6Sb_8S_{21}$ [23] and $Cu_{14}Sb_4S_{13}$ [32] were identified by using X-ray powder diffraction patterns. We have been able to synthesize $Tm_4Sb_2Se_{11.68}$ with the latter synthetic approach. Using Ag instead of Cu, the title compounds were still obtained with approximately the same yield.

2.2. X-ray powder diffraction

The phase identification was performed utilizing a Scintag theta-theta diffractometer equipped with a diffracted-beamed monochromatic set for Cu-K_α (λ=1.5418 Å). The powder patterns were collected at room temperature in scanning width of 0.03° and a fixed counting time of 1 s/step in 2θ range between 5 and 90°. These patterns were compared with those contained in DIFFRACplus EVA data-base [33].

2.3. Elemental analysis

The elemental analyses of Yb/Tm, Sb and S/Se have been examined on the field emission scanning electron microprobe (LEO EVO 50) equipped with an Oxford INCA Energy Dispersive X-ray Spectrometer (EDX). No cerium was detected and, neither copper nor silver elements were found in either compound as well. Moreover, wavelength-dispersive spectrometry WDX does not indicate the presence of Na or Br in the compounds.

2.4. Solid state UV/VIS analysis

The optical diffuse reflectance spectra of the title compounds were performed on the single crystals at room temperature using a Craic Technologies UV–VIS–NIR microspectrometer with the devise operating in the 300–1400 nm region. The reflectance data collected were used to estimate the material's band gap as reflectance are converted into absorption via the Kubelka–Munk function: $\alpha/S=(1-R)^2/2R$, where α is absorption coefficient, S the scattering coefficient and R the reflectance.

2.5. Crystal structure determination

The crystal data collections were performed at room temperature on a Bruker APEXII CCD X-ray diffractometer using graphite-monochromatized Mo-K_α radiation. SAINT software [34] was used for data integration including Lorentz and polarization corrections. The absorption corrections were done using SADABS program. The structure solution and refinement for both compounds

Table 1
Crystallographic data for $Yb_4Sb_2S_{11.25}$ and $Tm_4Sb_2Se_{11.68}$.

Compound		$Yb_4Sb_2S_{11.25}$	$Tm_4Sb_2Se_{11.68}$
Crystal system		Orthorhombic	Orthorhombic
Space group		*Pnnm* (no. 58)	*Pnnm* (no. 58)
Unit cell parameters[a)],	a/Å	12.446(2)	13.126 (2)
	b/Å	5.341(2)	5.623(1)
	c/Å	12.058(2)	12.499(2)
Formula unit per unit cell (Z)		2	2
Calculated density[a)] (D_x in g/cm^3)		5.37	6.66
Molar volume[a)] (V_m in cm^3/mol)		241.34	277.77
Index range ($\pm h_{max}$ / $\pm k_{max}$ / $\pm l_{max}$)		16/6/15	17/7/16
$2\theta_{max}$ (in deg)		55.00	54.99
F [0 0 0]		1123	1558
Absorption coefficient (μ in mm^{-1})		27.85	45.03
Collected reflections		12330	4693
Unique reflections		967	1105
R_{int}/R_σ		0.055/0.023	0.032/0.029
Reflections with $\lvert F_o\rvert \geq 4\sigma(F_o)$		820	920
R_1/R_1 with $\lvert F_o\rvert \geq 4\sigma(F_o)$		0.026/0.018	0.038/0.030
wR_2 (for all reflections)		0.040	0.0819
Goodness of Fit (GooF)		1.055	1.062
Residual electron density(max./min.) (ρ in e$^-$ 10^6 pm^{-3})		0.98/−1.05	3.11/−1.54

Table 2
Atomic coordinates and equivalent isotropic thermal displacement parameters (U_{eq}/Å^2) for $Yb_4Sb_2S_{11.25}$.

Atoms	Sof	Wyckoff site	x/a	y/b	z/c	U_{eq}[a]
Sb	1	4g	0.34297(14)	0.05220(10)	$^1/_2$	0.0099(1)
Yb	1	8h	0.34927(2)	−0.00489(3)	0.83789(2)	0.0090(1)
S1	1	4g	0.29766(14)	0.50113(27)	$^1/_2$	0.0102(4)
S2	1	8h	0.21263(10)	−0.00182(19)	0.34528(10)	0.0093(3)
S3	1	8h	0.50300(9)	−0.19735(22)	0.70360(11)	0.0120(3)
S4	0.76	2d	$^1/_2$	0	0	0.0189(8)
S5	0.24	4g	0.4990(5)	0.1991(14)	0	0.0131(15)

[a] U_{eq} is defined as one-third of the trace of orthogonalized U_{ij} tensor.

Table 3
Atomic coordinates and equivalent isotropic thermal displacement parameters (U_{eq}/Å^2) for $Tm_4Sb_2Se_{11.68}$.

Atoms	sof	Wyckoff site	x/a	y/b	z/c	U_{eq}[a]
Sb	0.70	4g	0.33902(11)	0.05831(26)	$^1/_2$	0.0103(3)
Tm	1	8h	0.35160(3)	−0.00357(6)	0.83551(3)	0.0135(2)
Se1	1	4g	0.29609(9)	0.50435(17)	$^1/_2$	0.0127(3)
Se2	1	8h	0.21043(7)	−0.00140(12)	0.34192(6)	0.0120(2)
Se3	1	8h	0.50247(6)	−0.21314(15)	0.69658(7)	0.0177(3)
Se4	0.30	2d	$^1/_2$	0	0	0.0243(15)
Se5	0.7	4g	0.5002(2)	0.2135(4)	0	0.0261(4)
SbA	0.30	4g	0.3550(5)	−0.0160(9)	$^1/_2$	0.0464(19)

[a] U_{eq} is defined as one-third of the trace of orthogonalized U_{ij} tensor.

Table 4
Selected interatomic distances (d/Å) and angles (∢ in deg) in $Yb_4Sb_2S_{11.25}$ and $Tm_4Sb_2Se_{11.68}$.

Yb	S1	2.677(1)	Tm	Se1	2.826(1)
	S2	2.765(1)		Se2	2.890(1)
	S2′	2.787(1)		Se2′	2.917(1)
	S2″	2.797(1)		Se2″	2.940(1)
	S3	2.678(1)		Se3	2.859(1)
	S3′	2.709(1)		Se3′	2.885(1)
	S4	2.709(1)		Se4	2.832(1)
	S5	2.912(2)		Se5	3.067(2)
Sb	S1	2.466(2)	Sb	Se1	2.571(2)
	S2 (× 2)	2.497(1)		Se2 (× 2)	2.620(1)
	S1′	2.999(2)		Se1′	3.175(2)
	S3 (× 2)	3.202(2)		Se3 (× 2)	3.321(2)
	S3′ (× 2)	3.424(2)		SbA–Se1	2.811(6)
	–			Se2 (× 2)	2.741(5)
				Se1	3.027(6)
				Se3 (× 2)	3.321(6)
				Se3′ (× 2)	3.345(6)
S3	S3	2.110(2)	Se3	Se3	2.398(2)
S5	S5	2.127(2)	Se5	Se5	2.401(4)
	S1–Sb–S2	87.68(4)		Se1–Sb–Se2	89.07(5)
	S2–Sb–S2	96.69(6)		Se2–Sb–Se2	97.89(6)
	Yb–S3–Yb (× 2)	88.31(4)		Tm–Se3–Tm (× 2)	85.42(3)
	Yb–S4–Yb	90.07(6)		Tm–Se4–Tm	89.51(6)

were performed with the aid of the SHELXTL package of crystallographic programs [35]. The complete data collection parameters, and details of the structure solutions and refinements are summarized in Table 1, while in Tables 2 and 3 the positional coordinates and isotropic equivalent thermal parameters for $Yb_4Sb_2S_{11.25}$ and $Tm_4Sb_2Se_{11.68}$ are, respectively given. (Table 4).

3. Results

The dark red and dark brown crystals of $Yb_4Sb_2S_{11.25}$ and $Tm_4Sb_2Se_{11.68}$, respectively, were found, and both crystallize orthorhombically in the same space group *Pnnm*. Their crystal structures are almost the same with a specific difference on the distribution of antimony (III) cations and the disordered dichalcogenide anions. We will only describe the crystal structure of the sulfide compound and the main difference with the selenide representative will be presented in the discussion section. The $Yb_4Sb_2S_{11.25}$ compound contains seven crystallographically different atom positions occupied by one Yb^{3+} and one Sb^{3+} cations together with five anions. However, the S4 and S5 atomic positions, which are very close each other (1.08 Å), are disordered, while at the S3 site are the disulfide $(S_2)^{2-}$ anions. This crystal structure is a three-dimensional tunnel framework dominated by the Yb–S polyhedra. Each Yb^{3+} cation is surrounded by four sulfide anions, one disulfide anion, and either another sulfide anion or a disulfide anion (in the 0.76/0.24 ratio) in a distorted pentagonal bipyramid (CN=7) or in a bicapped trigonal prism (CN=8). Four Yb–S polyhedra share square-(with Q5), triangular - faces and edges to form a tetramer $[Yb_4S_{19.25}]^{22-}$ building units (Fig. 1 *left*), which further connect to each other via eight corners of S2 to form infinite $[Yb_4S_{15.25}]^{14-}$ ribbons running along the short *b*-axis (Fig. 1 *right*). Those ribbons share common S2–S2 edges to form a three-dimensional $^3_\infty\{[Yb_4S_{11.25}]^{6-}\}$ framework with tunnels capable of embedding the Sb^{3+} cations (Fig. 2). The latter cations are surrounded by three sulfides ions in trigonal pyramid shape $[SbS_3]^{3-}$ (d(Sb–S=2.45–2.50 Å) and these polyhedra coordination number increase to 1+2+2 taking the weak contacts at 3.11, 3.21 and 3.43 Å, respectively in consideration. The Sb–S polyhedra build by the first and second coordination spheres form anionic $^1_\infty\{[SbS_3]^{3-}\}$ chains propagating along [0 1 0] (Fig. 3, *left above*), but with the third and fourth contact,

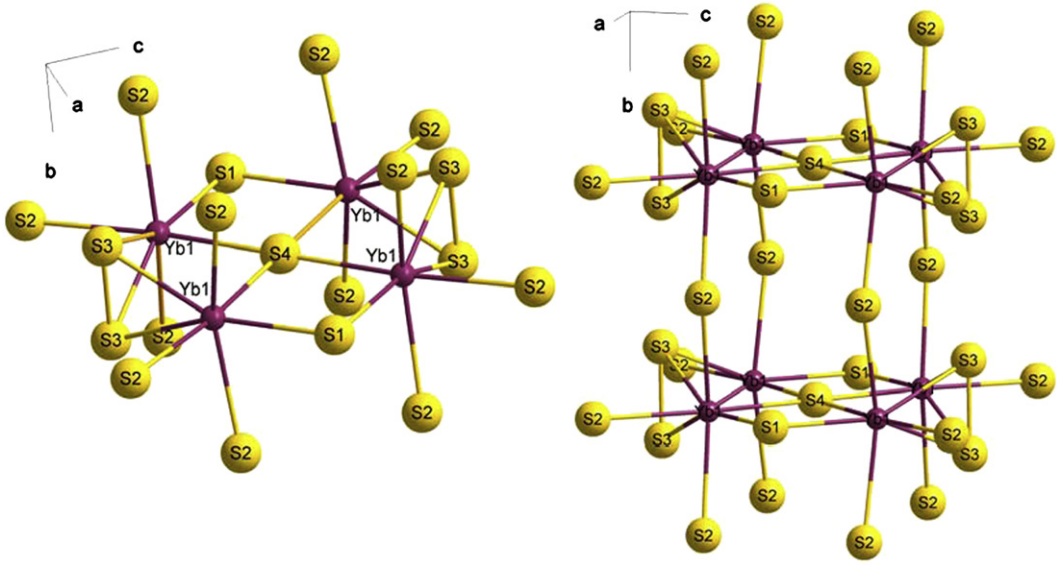

Fig. 1. The different connectivity models for Yb–S polyhedra in $Yb_4Sb_2S_{11.25}$ where disordered S5 atoms are omitted for clarity.

Sb^{3+} cations are surrounded by four sulfide and two disulfide anions to form $^{1}_{\infty}\{[Sb_2S_{10}]^{10-}\}$ double chains propagating along [0 1 0] (Fig. 3, *right*). The increasing of molar volume of the titled compounds (V_mSe/V_mS=1.15) is proportional to that of sulfur and selenium atomic radii ($r_{Se}/r_S \approx 1.17$).

The UV–VIS spectra obtained from these compounds show that they are both semi-conductors, with band gap values of 1.71 eV and 1.21 eV for $Yb_4Sb_2S_{11.25}$ and $Tm_4Sb_2Se_{11.68}$, respectively (Fig. 4). The sulfide value is comparable with that of Sb_2S_3 [36] and that agrees well with the dark red color of the crystals, however it is still larger than that of $Sm_2Mn_3Sb_4S_{12}$ (1.55 eV) or that of $La_4FeSb_2S_{10}$ (1.00 eV) [25,26]. The selenide compound band gap of 1.21 eV has almost the same value with $K_2Pr_{1.67}Sb_{4.33}Se_{12}$ (1.25 eV) [27] and is consistent with the dark brown color of the crystals. The absorption peak near 1.2 eV is attributed to a f–f transition and is frequently observed on lanthanide-chalcogenide UV–VIS spectrum.

4. Discussion

The $Yb_4Sb_2S_{11.25}$ crystal structure is comparable to that of RbU_2SbS_8 [37], where the cationic layers of (RbSb)U_2S_4 are alternatingly stacked with the disulfide anions layers perpendicularly to the *c*-axis. Identically here, the $Yb_4Sb_2S_6$ cationic layers and the almost dichalcogenide anionic layers (made of Q3 Q4 and Q5) are alternatingly stacked parallel to the *a*-axis. All the Yb–S distances found in $Yb_4Sb_2S_{11.25}$ are between 2.67 and 2.92 Å, which are in good agreement with those of 2.63–2.75 Å in $CuYbS_2$ [38]. Also, the Tm–Se lengths of 2.83–3.10 Å are comparable with those of 2.81–2.84 Å in $SrCuTmSe_3$ [39]. The existence of dichalcogenide in these two compounds justify the larger values of Ln–Q and can be confirmed by the presence of two relatively close Q3–Q3 chalcogen atoms, notably S–S at 2.11 and Se–Se at 2.40 Å apart. Similar distances have been found in the following compounds: La_2CuS_4 [40] where *d*(S–S)= 2.14 Å, $BaLaBi_2S_6$ [41] with *d*(S–S)=2.14 Å, $K_2La_2Sb_2S_9$ [28] with *d*(S–S)=2.12 Å, $KThSb_2Se_6$ [41] with *d*(Se–Se)=2.49 Å and $K_2Gd_2Sb_2Se_9$ [28] with *d*(Se–Se)=2.41 Å. The frequent presence of dichalcogenide or trichalcogenide in many lanthanide–antimony–chalcogenides systems may probably contribute to their stability. Their presence also satisfy the general formulae, assuming that lanthanides and antimony cations are trivalent, so, base on Wyckoff site position and s.o.f. these compounds general formulae can been written as $Yb_4Sb_2(S_2)_{2.25}S_{6.75}$ and $Tm_4Sb_2(Se_2)_{2.68}Se_{6.32}$. In both compounds, the antimony–chalcogenide $[SbQ_3]^{3-}$ polyhedra still exhibit stereochemical activities of lone pair of electrons as all are pointed toward the large tunnels, but that of the sulfide remains more distinctive. The shorter Sb–S distances of 2.46–2.50 Å are all in the average of those of known compounds such as $Pb_3Sb_8S_{15}$ [42] or $Cs_2Sb_4S_7$ (*d*(Sb–S)=2.39–2.86 Å) [43] with coordination numbers 3 or 3+1, but even when they increase to 5 like in Sb_2S_3 (*d*(Sb–S)=2.45–3.11 Å) [31] or 6 in $K_2La_2Sb_2S_9$ (*d*(Sb–S)=2.46–3.20 Å), the distances expand slightly, while in the titled sulfide they are larger () due to disulfide weak interaction. However, the Sb^{3+} cations in the selenide compound are disordered over two main positions named here Sb and SbA with Sb–Se range between 2.57 and 2.63 Å while SbA–Se range between 2.74 and 2.81 Å, with next contacts found at 3.17 and

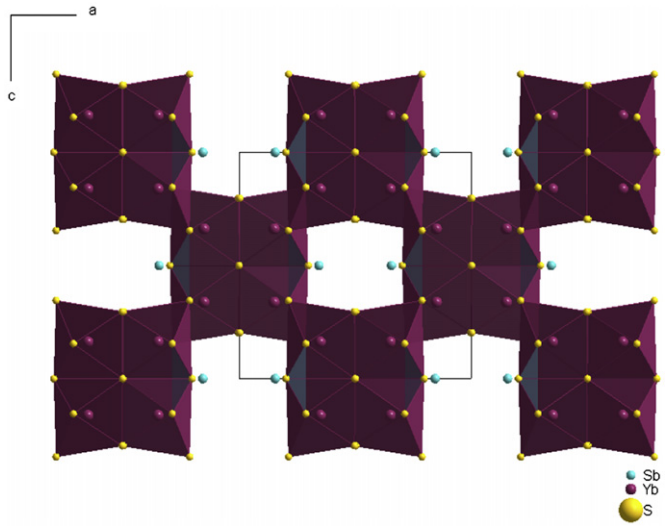

Fig. 2. The crystal structure of $Yb_4Sb_2S_{11.25}$ viewed along the [0 1 0].

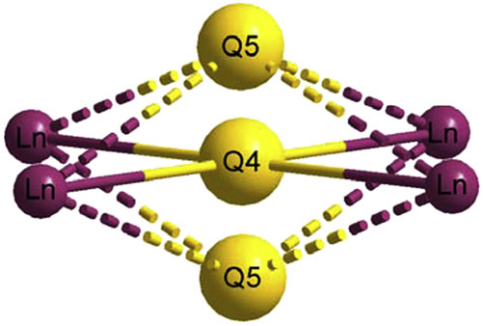

Fig. 4. The Q4 and Q5 coordination environments in both compounds.

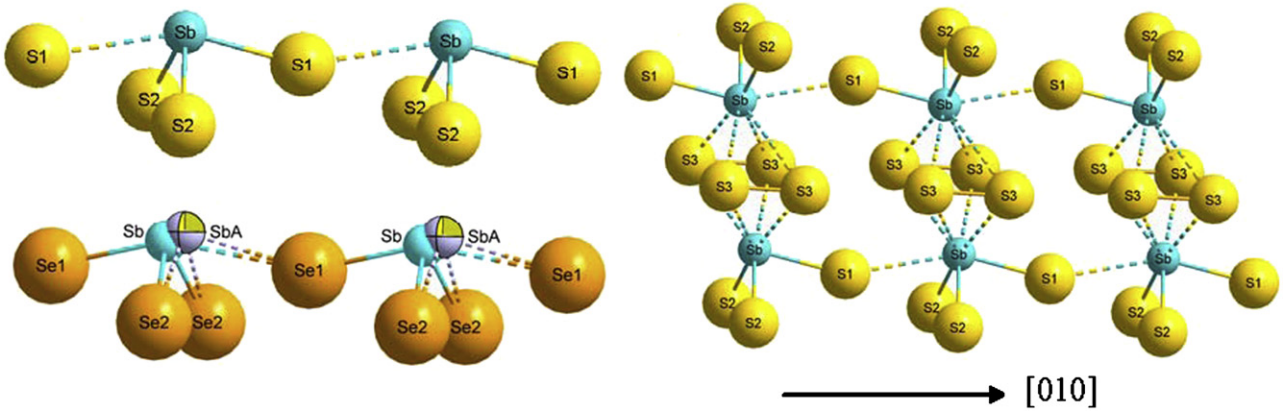

Fig. 3. The $[SbS_3]^{3-}$ unit connected through a secondary contact into chain (*left*, *above*) with the two disordered positions for antimony in $Tm_4Sb_2Se_{11.68}$ (*left*, *below*) within the chain, and the resulting double chain form by the $[Sb_2S_{12}]^{14-}$ all running along *b*-axis (*right*).

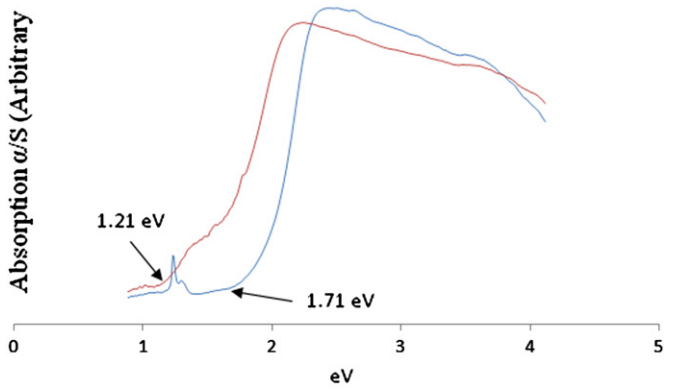

Fig. 5. The UV–VIS diffuse reflectance of $Yb_4Sb_2S_{11.25}$ (*red*) and $Tm_4Sb_2Se_{11.68}$ (*blue*).

3.02 Å, respectively. These two crystallographically different sites situated at 0.47 Å apart are positioned in a large eightfold coordination environment made of four selenides and two diselenides anions. The antimony cations at SbA site (with less occupancy) depict relative larger distances (2.74–2.81 Å), but have the secondary contact at 3.02 Å which is closer than that at 3.17 Å to the Sb. This behavior is common to antimony-chalcogenides as found in $K_2La_2Sb_2S_9$ and $K_2Gd_2Sb_2Se_9$ where similar expanded-distances (Sb2–Q) were also found. But the later was observed in both isotypical sulfide and selenide, while is found here only in selenide. These compounds have in common Sb disordered over two different but close sites, which can explain those expansions. A relatively high residual electron density was found between Sb and SbA (0.59 Å to SbA and 0.88 Å to Sb), that can explain the presence of lone pair electrons. The large isotropic thermal displacements for the SbA atoms as well as all the Q4 and Q5 are consequent with disordering. The chalcogenides at Q1 and Q2 show a common tetrahedral environment; whereas those at Q4 and Q5 and the dichalcogenides at Q3 positions exhibit unusual surroundings. Q4 is the center of square formed by four lanthanides (Ln), meanwhile the Q5 position is either the top or the bottom of the above square which results in a square bipyramidal shaped polyhedron (see Fig. 5). The Q5–Q5 distances of 2.13 Å for sulfide and 2.40 Å for selenide are equivalent to those of respective dichalcogenides, suggesting the existence of extra anions of that specie. Moreover, the ratio S4/S5 ≈ Se5/Se4 shows that the selenide compound has more dichalcogenide anions enhancing the difference in general formula of the titled compounds. While the dichalcogenide ions found at Q3 just bridge two Ln–Q polyhedral (Fig. 1) in edge-sharing connection and with angles Ln–(Q_2)–Ln of 88.3 and 85.4° for sulfide and selenide, respectively, the extra dichalcogenides anions at Q5 site position form with four lanthanide cations Ln^{3+} an unusual cationic [Q_2Ln_4] octahedron. One unusual dichalcogenide anions bridging polyhedral have been reported in La_2CuS_4 [40] where $(S_2)^{2-}$ anions bind two triangular $[CuS_3]^{5-}$ units through corner-sharing to form discrete building unit, contrary to those of the title compounds which are further connected into a framework.

5. Conclusions

Two new lanthanide antimony chalcogenides have been synthesized and characterized both structurally and optically. Both compounds are non-stoichiometric, wide band gap semiconductors with tunnel structures. Their structure types are novel and chalcogen connectivity and polyhedra are atypical for this series.

Supporting information available

Further details of the crystal structure investigation may be obtained from the Fachinformationzentrum Karlsruhe, D-76344 Eggenstein-Leopoldshafen, Germany (crysdata@fiz-karlsruhe.de) on quoting numbers 423575 and 423576.

Acknowledgment

This work was supported by the National Science Foundation, Division of Materials Research, through DMR-1004459.

Appendix A. Supplementary materials

Supplementary materials associated with this article can be found in the online version at doi:10.1016/j.jssc.2012.01.020.

References

[1] R. Venkatasubramanian, E. Slivola, T. Colpitts, B. O'Quinn, Nature 413 (2001) 597.
[2] Y. Hermodsson, Acta Chem. Scand. 21 (1967) 1313.
[3] A. Edenharter, W. Nowacki, Y. Takeuchi, Z. Kristallogr. 131 (1970) 397.
[4] R.J. Gillepsie, E. Maharajh, W.C. Luk, D.R. Slim, Inorg. Chem. 16 (1977) 892.
[5] K. Volk, H. Schaefer, Z. Naturforsch. 34 b (1979) 1637.
[6] R.C. Burns, W.L. Chan, R.J. Gillepsie, W.C. Luk, J.F. Sawyer, D.R. Slim, Inorg. Chem. 19 (1980) 1432.
[7] M. Gostojic, W. Nowacki, P. Engel, Z. Kristallogr. 159 (1982) 217.
[8] J. Zhou, G.-Q. Bian, Q.-Y. Zhu, Y. Zhang, C.-Y. Li, J. Dai, J. Solid State Chem. 182 (2009) 259.
[9] M. Palazzi, S. Jaulmes, P. Laruelle, Acta Crystallogr. B 30 (1974) 2378.
[10] G. Adiwidjaja, J. Loehn, Acta Crystallogr. B 26 (1970) 1878.
[11] P.T. Wood, G.L. Schimek, J.W. Kolis, Chem. Mater. 8 (1996) 721.
[12] S. Loeken, W. Tremel, Eur. J. Inorg. Chem. 1998 (1998) 283.
[13] A. Gagor, A. Pawlowski, A. Pietraszko, J. Solid State Chem. 182 (2009) 451.
[14] Y.-D. Wu, C. Naether, W. Bensch, Inorg. Chem. 22 (2006) 8835.
[15] A. Heerwig, M. Ruck, Z. Anorg. Allg. Chem. 636 (2010) 1860.
[16] D. Topa, E. Makovicky, H. Putz, Can. Mineral. 48 (2010) 145.
[17] D. Topa, E. Makovicky, T. Balic-Zunic, Can. Mineral. 40 (2002) 1147; D. Topa, V. Petricek, M. Dusek, E. Makovicky, T. Balic-Zunic, Can. Mineral. 46 (2008) 525.
[18] E. Makovicky, I. Sotofte, S. Karup-Moller, Z. Kristallogr. 217 (2002) 597.
[19] P. Lemoine, D. Carre, M. Guittard, Acta Crystallogr. B 37 (1981) 1281.
[20] G.B. Jin, D.M. Wells, S.J. Crerar, T.C. Shehee, A. Mar, T.E. Albrecht-Schmitt, Acta Crystallogr. E 61 (2005) i116.
[21] D.-H. Kang, Th. Schleid, Z. Anorg. Allg. Chem. 635 (2009) 2170.
[22] G.G. Guseinov, F.K. Mamedov, I.R. Amiraslanov, K.S. Mamedov, Sov. Phys. Crystallogr. 26 (1981) 470.
[23] J.Z. Gao, I. Nakai, K. Nagashima, Bull. Chem. Soc. Jpn. 57 (1984) 875.
[24] A. Assoud, K.M. Kleinke, H. Kleinke, Chem. Mater. 18 (2006) 1041.
[25] H.-J. Zhao, L.-H. Li, L.-M. Wu, L. Chen, Inorg. Chem. 49 (2010) 5811.
[26] H.-J. Zhao, L.-H. Li, L.-M. Wu, L. Chen, Inorg. Chem. 48 (2009) 11518.
[27] J.H. Chen, P.K. Dorhout, J. Alloys Compd. 249 (1997) 199.
[28] K.-S. Choi, J.A. Hanko, M.G. Kanatzidis, J. Solid State Chem. 147 (1999) 309.
[29] G. Gauthier, M. Evain, S. Jobic, R. Brec, Solid State Sci. 4 (2002) 1361.
[30] J.A. Aitken, K. Chondroudis, V.G. Young Jr., M.G. Kanatzidis, Inorg. Chem. 39 (2000) 1525.
[31] W. Hofmann, Z. Kristallogr. 86 (1933) 225.
[32] L. Calvert, National Research Council of Canada, Ottawa, Canada 1980.
[33] DIFFRACplus E.V.A. is part of DIFFRACplus BASIC package from BRUKER AXS, INC, Madison WI, USA 2002.
[34] SAINT: version 4, Siemens Analytical X-ray Systems, Inc, Madison WI, 1996.
[35] SHELXTL: version 5, G.M. Sheldrick, Siemens Analytical X-ray Systems, Inc, Madison WI, USA 1997.
[36] S.D. Shutov, V.V. Sobolev, Y.V. Popov, S.N. Shestaskii, Phys. Status Solidi 31 (1969) K23.
[37] K.-S. Choi, M.G. Kanatzidis, Chem. Mater. 11 (1999) 2613.
[38] S. Strobel, Th. Schleid, Z. Naturforsch. 62 b (2007) 15.
[39] S. Strobel, Dissertation, University of Stuttgart, Germany 2004.
[40] Strobel, Th. Schleid, Angew. Chem. Int. Ed. 42 (2003) 4911.
[41] K.-S. Choi, L. Iordanidis, K. Chondroudis, M.G. Kanatzidis, Inorg. Chem. 36 (1997) 3804.
[42] E.W. Nuffield, Acta Crystallogr. B 31 (1975) 151.
[43] G. Dittmar, H. Schaefer, Z. Anorg. Allg. Chem. 441 (1978) 98.